2005 American Control Conference
June 8-10, 2005. Portland, OR, USA

Motion Estimation of Plane Polynomial Curves

Mustafa Unel and Bijoy K. Ghosh

Abstract— **In this paper, we are interested in the motion estimation of a planar free-form object whose boundary is represented by a plane polynomial curve. We develop new Riccati equations in real variables for the slope and intercept parameters of the line factors obtained from the decomposition of the closed-bounded polynomial curve. We also derive new recursions on multiplicative scalars of the decomposition. For the estimation of motion parameters, an adaptive scheme has been employed and the results are verified by simulations.**

I. INTRODUCTION

Implicit polynomial curves have proven very useful in many model-based applications. Various algebraic and geometric invariants obtained from implicit models of curves have been studied rather extensively in Computer Vision, especially for single computation pose estimation, shape tracking, 3D surface estimation from multiple images and efficient geometric indexing of large pictorial databases [1]- [13]. Such curves might originate as features that are observed by the aid of a charged coupled device camera (CCD), or they might originate as the outline of a surface being observed with the aid of a laser range finder (LRF), see Fig. 1. In either of the two cases, one is typically faced with the problem of modelling two dimensional planar curves in motion.

Free-form objects usually do not have any visual features such as corners or some other easily distinguishable points, so that one can establish correspondence among these points in subsequent images. However, object boundaries can be represented by plane polynomial curves and these curves can be simplified through polynomial decompositions [5]. It was shown in an earlier paper [8] that rigid or affine dynamics of plane polynomial curves can be represented in terms of Riccati dynamics of possibly complex lines obtained from curve decompositions. The application of this result was illustrated for planar curves moving in $\mathbb{R}^3$ and for the perspective projections of these curves on the image plane of a CCD camera. In this paper, we develop new Riccati equations in real variables for closed-bounded curves and obtain some new recursions on parameters. We also propose an adaptive identification scheme for estimating the rigid motion parameters of a plane polynomial curve using the parameters of the line factors. We illustrate the validity of our proposed approach by simulations. There has been a steadily growing literature in robotics on the problem of line correspondence for line features moving in $\mathbb{R}^3$, (see [14]- [18]). For some other older references in the literature on the dynamics of curves, see [19]- [21].

The second author would like to acknowledge the support from NSF grants ECS-9976174, and ECS-0323693.

M. Unel is with the Faculty of Engineering and Natural Sciences, Sabanci University, Tuzla 34956, Istanbul, Turkey munel@sabanciuniv.edu

B. K. Ghosh is with the Department of Electrical and Systems Engineering, Washington University, St. Louis, MO 63130, USA ghosh@netra.wustl.edu

II. PLANE POLYNOMIAL CURVES AND ASYMPTOTES

Plane polynomial or so called algebraic curves are defined by implicit equations of the form $f(x,y)=0$, where $f(x,y)$ is a polynomial in the variables x,y, i.e. $f(x,y)=\sum_{ij}a_{ij}x^iy^j$ where $0\le i+j\le n$ (n is finite) and the coefficients a_{ij} are real numbers [1]. Alternatively, the intersection of an explicit surface $z=f(x,y)$ with the $z=0$ plane yields a plane polynomial curve if $f(x,y)$ is a polynomial. Algebraic curves of degree 1, 2, 3, 4, …are called *lines, conics, cubics, quartics,* …etc.

In general, a *plane polynomial curve* of *degree n* can be defined by the *implicit polynomial (IP) equation*:

$$f_n(x,y)=\underbrace{a_{00}}_{H_0}+\underbrace{a_{10}x+a_{01}y}_{H_1(x,y)}+\underbrace{a_{20}x^2+a_{11}xy+a_{02}y^2}_{H_2(x,y)}+\ldots$$

$$+\underbrace{a_{n0}x^n+a_{n-1,1}x^{n-1}y+\ldots+a_{0n}y^n}_{H_n(x,y)}=\sum_{i=0}^{n}H_i(x,y)=0, \quad (1)$$

where each binary *form* $H_r(x,y)$ is a *homogeneous polynomial* of degree r in the variables x and y. The number of terms in each $H_r(x,y)$ is $r+1$, so that the IP equation defined by (1) has one constant term, two terms of the first degree, three terms of the second degree, etc., up to and including $n+1$ terms of the (highest) n-th degree, for a total of $(n+1)(n+2)/2$ coefficients. Since the above equation can be multiplied by a non-zero constant without changing the zero set, an algebraic curve defined by $f_n(x,y)=0$ has $(n+1)(n+2)/2-1=n(n+3)/2$ independent coefficients or *degrees of freedom* (DOF). A *monic* polynomial $f_n(x,y)=0$ will be defined by the condition that $a_{n0}=1$ in (1).

We next note that an *asymptote* to the curve $f_n(x,y)=0$ is a tangent line $y=mx+b$ which intersects the curve at infinity [2]. Asymptotes can be determined by substituting $y=mx+b$ for y in (1) and writing the highest degree terms first, so that

$$\begin{aligned}f_n(x,y)&=\{a_{n0}+a_{n-1,1}m+\ldots+a_{0n}m^n\}x^n\\&+\{[a_{n-1,0}+a_{n-2,1}m+\ldots+a_{0,n-1}m^{n-1}]\\&+b[a_{n-1,1}+2a_{n-2,2}m+\ldots+na_{0n}m^{n-1}]\}x^{n-1}+\ldots\\&=H_n(m)x^n+\{\underbrace{H_{n-1,0}(m)+bH_{n-1,1}(m)}_{H_{n-1}(m,b)}\}x^{n-1}+\ldots\end{aligned}$$

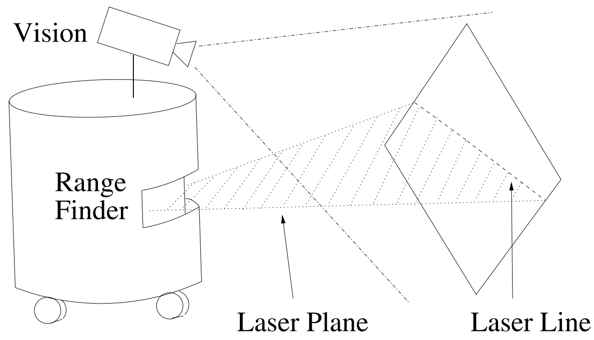

Fig. 1. The Laser Range Finder and the CCD vision

The line $y = mx + b$ will be an asymptote if both $H_n(m) = 0$ and $H_{n-1}(m,b) = 0$, since the curve will then have two roots at infinity, corresponding to two intersections with the asymptote there. Any line parallel to an asymptote $y = mx + b$, such as $y = mx$, will intersect the curve once at infinity, since (only) $H_n(m) = 0$. Each real root m_i of $H_n(m)$ will then imply a corresponding real asymptote defined by the line $y = m_i x + b_i$, with $b_i = -H_{n-1,0}(m_i)/H_{n-1,1}(m_i)$.

In general, $H_n(m) = 0$ will have n roots, which may be complex (conjugates) or real. $H_n(m) = 0$ will have at least one real root when n is odd, so that *odd curves are unbounded. Even degree curves* may or may not have real asymptotes. For example, an ellipse is an even degree curve and it has no real asymptote and therefore it is closed-bounded. On the other hand, a hyperbola, although it is an even degree curve, has two real asymptotes and therefore it is unbounded.

Therefore, to represent 2-D closed and bounded curves, IPs of even degree must be used. For a bounded (even) IP curve, $H_n(m) = 0$ will have exactly $p = n/2$ pairs of complex conjugate roots.

Free-form object boundaries can be represented by polynomial curves of varying degrees. Higher degree representations imply better shape representation capability. However, it is not practical to use very high degree curves because of the numerical stability problems. Therefore one idea might be to start with the lowest degree polynomials such as conics. However real life objects are too complicated to be modelled by conics. So we next consider quartics which are the 4th degree curves. Quartic curves can represent a variety of different free form objects that are too complicated to be represented by circles or ellipses. Fig. 2 depicts the boundaries of several *free-form* objects with superimposed plane quartic curves.

In this work we will restrict our attention to quartics and note that results can easily be generalized to higher curves.

III. LINE DECOMPOSED QUARTICS AND RICCATI EQUATIONS

As detailed in [5], [7], plane polynomial curves can be decomposed as a *unique* sum of *line products*. Example of a quartic decomposition in terms of 6 complex lines is geometrically shown in Fig. 2.

In [8], we considered a line decomposed planar quartic curve

$$f_4(x,y) = \prod_{i=1}^{4} \begin{pmatrix} 1 & l_{4i} & k_{4i} \end{pmatrix} \begin{pmatrix} x \\ y \\ 1 \end{pmatrix} + \alpha \prod_{i=1}^{2} \begin{pmatrix} 1 & l_{2i} & k_{2i} \end{pmatrix} \begin{pmatrix} x \\ y \\ 1 \end{pmatrix} + \beta = 0 \qquad (2)$$

and its homogenized version, namely

$$f_4(\bar{x},\bar{y},\bar{w}) = \prod_{i=1}^{4} \begin{pmatrix} \bar{p}_i & \bar{l}_{4i} & \bar{k}_{4i} \end{pmatrix} \begin{pmatrix} \bar{x} \\ \bar{y} \\ \bar{w} \end{pmatrix} + \alpha\left(\frac{\prod_{i=1}^{4} \bar{p}_i}{\prod_{i=1}^{2} \bar{q}_i}\right)\bar{w}^2 \prod_{i=1}^{2} \begin{pmatrix} \bar{q}_i & \bar{l}_{2i} & \bar{k}_{2i} \end{pmatrix} \begin{pmatrix} \bar{x} \\ \bar{y} \\ \bar{w} \end{pmatrix} + \beta\left(\prod_{i=1}^{4} \bar{p}_i\right)\bar{w}^4 = 0 \qquad (3)$$

obtained from (2) by using the following substitutions:

$$x = \frac{\bar{x}}{\bar{w}},\ y = \frac{\bar{y}}{\bar{w}},\ l_{4i} = \frac{\bar{l}_{4i}}{\bar{p}_i},\ k_{4i} = \frac{\bar{k}_{4i}}{\bar{p}_i},\quad l_{2i} = \frac{\bar{l}_{2i}}{\bar{q}_i},\ k_{2i} = \frac{\bar{k}_{2i}}{\bar{q}_i} \qquad (4)$$

Let us now consider an affine motion in the cartesian and in the homogeneous coordinates as follows:

$$\frac{d}{dt}\begin{pmatrix} x \\ y \\ 1 \end{pmatrix} = \underbrace{\begin{pmatrix} a_1 & a_2 & b_1 \\ a_3 & a_4 & b_2 \\ 0 & 0 & 0 \end{pmatrix}}_{A} \begin{pmatrix} x \\ y \\ 1 \end{pmatrix} \Rightarrow$$

$$\frac{d}{dt}\begin{pmatrix} \bar{x} \\ \bar{y} \\ \bar{w} \end{pmatrix} = \underbrace{\begin{pmatrix} a_1 & a_2 & b_1 \\ a_3 & a_4 & b_2 \\ 0 & 0 & 0 \end{pmatrix}}_{A} \begin{pmatrix} \bar{x} \\ \bar{y} \\ \bar{w} \end{pmatrix} \qquad (5)$$

We obtain the following dynamics on the line parameters and on the coefficients $\alpha(t)$ and $\beta(t)$:

$$\frac{d}{dt}\begin{pmatrix} \bar{p}_i(t) \\ \bar{l}_{4i}(t) \\ \bar{k}_{4i}(t) \end{pmatrix} = -A^T \begin{pmatrix} \bar{p}_i(t) \\ \bar{l}_{4i}(t) \\ \bar{k}_{4i}(t) \end{pmatrix} = \begin{pmatrix} -a_1 & -a_3 & 0 \\ -a_2 & -a_4 & 0 \\ -b_1 & -b_2 & 0 \end{pmatrix} \begin{pmatrix} \bar{p}_i(t) \\ \bar{l}_{4i}(t) \\ \bar{k}_{4i}(t) \end{pmatrix} \quad i = 1,2,3,4 \qquad (6)$$

$$\frac{d}{dt}\begin{pmatrix} \bar{q}_i(t) \\ \bar{l}_{2i}(t) \\ \bar{k}_{2i}(t) \end{pmatrix} = -A^T \begin{pmatrix} \bar{q}_i(t) \\ \bar{l}_{2i}(t) \\ \bar{k}_{2i}(t) \end{pmatrix} = \begin{pmatrix} -a_1 & -a_3 & 0 \\ -a_2 & -a_4 & 0 \\ -b_1 & -b_2 & 0 \end{pmatrix} \begin{pmatrix} \bar{q}_i(t) \\ \bar{l}_{2i}(t) \\ \bar{k}_{2i}(t) \end{pmatrix} \quad i = 1,2. \qquad (7)$$

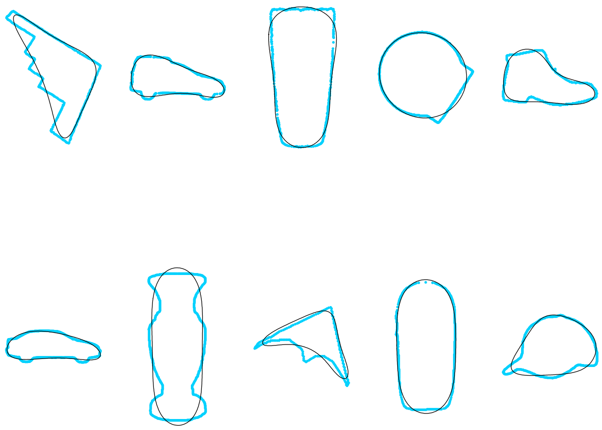

Fig. 2. A group of Quartic Curves as Outlines of Free-Form Objects: a plane, a van, a glass vaze, a CD box, a shoe, a car, another vaze, a glider, a cellular phone, and a hat in above order

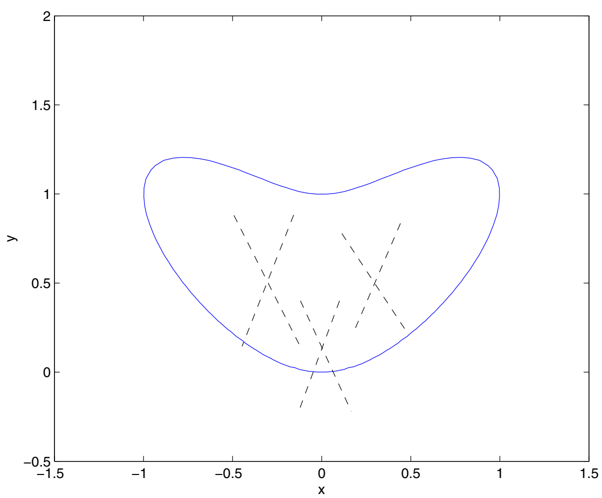

Fig. 3. A Boomerang Shaped Curve (Solid) and its Complex Line Factors (Dashed)

$$\alpha(t) = \left(\prod_{i=1}^{4} \frac{\bar{p}_i(0)}{\bar{p}_i(t)}\right)\left(\prod_{i=1}^{2} \frac{\bar{q}_i(t)}{\bar{q}_i(0)}\right)\alpha(0); \tag{8}$$

$$\beta(t) = \left(\prod_{i=1}^{4} \frac{\bar{p}_i(0)}{\bar{p}_i(t)}\right)\beta(0). \tag{9}$$

A. Riccati Equations

By differentiating (4) with respect to time and using (6) and (7), it has also been shown in [8] that line parameters $l_{4i}, k_{4i}, l_{2i}, k_{2i}$ in the decomposition of the original curve satisfy coupled Riccati equations, namely

$$\dot{l}_{4i} = -a_2 + (a_1 - a_4)l_{4i} + a_3 l_{4i}^2, \quad i = 1,2,3,4 \tag{10}$$

$$\dot{k}_{4i} = -b_1 - b_2 l_{4i} + a_1 k_{4i} + a_3 l_{4i} k_{4i}, \quad i = 1,2,3,4 \tag{11}$$

$$\dot{l}_{2i} = -a_2 + (a_1 - a_4)l_{2i} + a_3 l_{2i}^2, \quad i = 1,2 \tag{12}$$

$$\dot{k}_{2i} = -b_1 - b_2 l_{2i} + a_1 k_{2i} + a_3 l_{2i} k_{2i}, \quad i = 1,2 \tag{13}$$

Note that the line parameters, i.e. slope and intercept, satisfy coupled Riccati equations with parameters that depend on the motion of the curve. Note also that each of the lines satisfies the same Riccati Equation initialized at different points on the state space.

B. New Riccati Equations in Real Variables for Closed-Bounded Quartics

For a closed-bounded quartic curve, l_{4i} and k_{4i} have to be in complex conjugate pairs. Focusing on these:

$$l_{4i} = \xi_{1i} + j\xi_{2i}, \;\; k_{4i} = \xi_{3i} + j\xi_{4i}, \;\; i = 1,3 \tag{14}$$

where $\xi_{1i} = Re(l_{4i})$, $\xi_{2i} = Im(l_{4i})$, $\xi_{3i} = Re(k_{4i})$, $\xi_{4i} = Im(k_{4i})$, and

$$l_{4i} = \xi'_{1i} + j\xi'_{2i}, \;\; k_{4i} = \xi'_{3i} + j\xi'_{4i}, \;\; i = 2,4 \tag{15}$$

where $\xi'_{1i} = \xi_{1i}$, $\xi'_{2i} = -\xi_{2i}$, $\xi'_{3i} = \xi_{3i}$, $\xi'_{4i} = -\xi_{4i}$. Substituting these into (10) and (11),

$$\dot{l}_{4i} = \dot{\xi}_{1i} + j\dot{\xi}_{2i} = -a_2 + (a_1 - a_4)(\xi_{1i} + j\xi_{2i}) + a_3(\xi_{1i} + j\xi_{2i})^2$$

$$\Rightarrow \dot{\xi}_{1i} + j\dot{\xi}_{2i} = -a_2 + (a_1 - a_4)\xi_{1i} + a_3({\xi_{1i}}^2 - {\xi_{2i}}^2) +$$

$$j[(a_1 - a_4)\xi_{2i} + 2a_3\xi_{1i}\xi_{2i}]$$

Equating the real and the imaginary parts we obtain the following:

$$\dot{\xi}_{1i} = -a_2 + (a_1 - a_4)\xi_{1i} + a_3({\xi_{1i}}^2 - {\xi_{2i}}^2) \tag{16}$$

$$\dot{\xi}_{2i} = (a_1 - a_4)\xi_{2i} + 2a_3\xi_{1i}\xi_{2i} \tag{17}$$

Similarly, we also have the following

$$\dot{k}_{4i} = \dot{\xi}_{3i} + j\dot{\xi}_{4i} = -b_1 - b_2(\xi_{1i} + j\xi_{2i}) + a_1(\xi_{3i} + j\xi_{4i}) +$$

$$a_3(\xi_{1i} + j\xi_{2i})(\xi_{3i} + j\xi_{2i})$$

$$\dot{\xi}_{3i} + j\dot{\xi}_{4i} = -b_1 - b_2\xi_{1i} + a_1\xi_{3i} + a_3(\xi_{1i}\xi_{3i} - \xi_{2i}\xi_{4i}) +$$

$$j[-b_2\xi_{2i} + a_1\xi_{4i} + a_3(\xi_{1i}\xi_{4i} + \xi_{2i}\xi_{3i})]$$

As before, equating the real and the imaginary parts we have

$$\dot{\xi}_{3i} = -b_1 - b_2\xi_{1i} + a_1\xi_{3i} + a_3(\xi_{1i}\xi_{3i} - \xi_{2i}\xi_{4i}) \tag{18}$$

$$\dot{\xi}_{4i} = -b_2\xi_{2i} + a_1\xi_{4i} + a_3(\xi_{1i}\xi_{4i} + \xi_{2i}\xi_{3i}) \tag{19}$$

Likewise, for the conjugate variables ξ'_{1i} to ξ'_{4i} we obtain the following:

$$\dot{\xi}'_{1i} = -a_2 + (a_1 - a_4)\xi'_{1i} + a_3({\xi'_{1i}}^2 - {\xi'_{2i}}^2) \tag{20}$$

$$\dot{\xi}'_{2i} = (a_1 - a_4)\xi'_{2i} + 2a_3\xi'_{1i}\xi'_{2i} \tag{21}$$

$$\dot{\xi}'_{3i} = -b_1 - b_2\xi'_{1i} + a_1\xi'_{3i} + a_3(\xi'_{1i}\xi'_{3i} - \xi'_{2i}\xi'_{4i}) \tag{22}$$

$$\dot{\xi}'_{4i} = -b_2\xi'_{2i} + a_1\xi'_{4i} + a_3(\xi'_{1i}\xi'_{4i} + \xi'_{2i}\xi'_{3i}) \tag{23}$$

C. Recursion on Multiplicative Parameters

In light of (6) and (7),

$$\dot{\bar{p}}_i(t) = -a_1\bar{p}_i(t) - a_3\bar{l}_{4i}(t) \Rightarrow$$

$$\frac{\dot{\bar{p}}_i(t)}{\bar{p}_i(t)} = -a_1 - a_3\underbrace{\frac{\bar{l}_{4i}(t)}{\bar{p}_i(t)}}_{l_{4i}(t)} = -a_1 - a_3 l_{4i}(t)$$

Integrating both sides we have

$$\ln(\bar{p}_i(\mu))]_0^t = -\int_0^t (a_1 + a_3 l_{4i}(\mu))d\mu \Rightarrow$$

$$\frac{\bar{p}_i(t)}{\bar{p}_i(0)} = e^{-\int_0^t (a_1+a_3 l_{4i}(\mu))d\mu}$$

Similarly, from (7) we get

$$\frac{\bar{q}_i(t)}{\bar{q}_i(0)} = e^{-\int_0^t (a_1+a_3 l_{2i}(\mu))d\mu}$$

Finally from (8), (9) we conclude that

$$\alpha(t) = (\frac{\prod_{i=1}^4 e^{\int_0^t (a_1+a_3 l_{4i}(\mu))d\mu}}{\prod_{i=1}^2 e^{\int_0^t (a_1+a_3 l_{4i}(\mu))d\mu}})\alpha(0) =$$

$$e^{2a_1 t} e^{a_3 \int_0^t [\Sigma_{i=1}^4 l_{4i}(\mu) - \Sigma_{i=1}^2 l_{2i}(\mu)]d\mu}\alpha(0)$$

and

$$\beta(t) = (\prod_{i=1}^4 e^{\int_0^t (a_1+a_3 l_{4i}(\mu))d\mu})\beta(0)$$

$$= e^{4a_1 t} e^{a_3 \int_0^t [\Sigma_{i=1}^4 l_{4i}(\mu)]d\mu}\beta(0) \quad (24)$$

The above equation (24) can be written in the form of an ordinary differential equation as follows:

$$\dot{\alpha} = [2a_1 + a_3(\sum_{i=1}^4 l_{4i}(t) - \sum_{i=1}^2 l_{2i}(t))]\,\alpha$$

$$\dot{\beta} = [4a_1 + a_3(\sum_{i=1}^4 l_{4i}(t))]\,\beta$$

IV. ADAPTIVE ESTIMATION OF MOTION PARAMETERS

Using vector-matrix notation and dropping the subscript i, equations (16) to (19), or alternatively (20) to (23), for a specific complex conjugate line pair can be recast as

$$\begin{pmatrix} \dot{\xi}_1 \\ \dot{\xi}_2 \\ \dot{\xi}_3 \\ \dot{\xi}_4 \end{pmatrix} = \begin{pmatrix} (a_1-a_4) & 0 & 0 & 0 \\ 0 & (a_1-a_4) & 0 & 0 \\ -b_2 & 0 & a_1 & 0 \\ 0 & -b_2 & 0 & a_1 \end{pmatrix} \begin{pmatrix} \xi_1 \\ \xi_2 \\ \xi_3 \\ \xi_4 \end{pmatrix} +$$

$$a_3 \begin{pmatrix} \xi_1{}^2 - \xi_2{}^2 \\ 2\xi_1\xi_2 \\ \xi_1\xi_3 - \xi_2\xi_4 \\ \xi_1\xi_4 + \xi_2\xi_3 \end{pmatrix} + \begin{pmatrix} a_2 \\ 0 \\ b_1 \\ 0 \end{pmatrix}(-1) \quad (25)$$

which is a nonlinear plant of the form

$$\dot{X}_p = A_p X_p + C_p f(X_p) + B_p g(u) \quad (26)$$

where A_p, B_p and C_p are unknown constant matrices, $f(.)$ and $g(.)$ are known smooth functions of their arguments. Note in particular that $g(u) = -1$ is constant in our problem. To estimate the unknown parameters, we construct an estimator of the form [22]

$$\dot{\hat{X}}_p = A_m\hat{X}_p + (\hat{A}_p(t) - A_m)X_p + \hat{C}_p(t)f(X_p) + \hat{B}_p(t)g(u) \quad (27)$$

If the state error and parameter errors are defined as

$$e(t) \stackrel{def}{=} \hat{X}_p(t) - X_p(t), \ \Phi(t) \stackrel{def}{=} \hat{A}_p(t) - A_p,$$

$$\Psi(t) \stackrel{def}{=} \hat{C}_p(t) - C_p, \ \Gamma(t) \stackrel{def}{=} \hat{B}_p(t) - B_p,$$

then the error equations are given by

$$\dot{e}(t) = A_m e(t) + \Phi(t)X_p(t) + \Psi(t)f(X_p) + \Gamma(t)g(u), \quad (28)$$

where A_m is a stability matrix. The problem is to adjust the elements of the matrices $\hat{A}_p(t), \hat{C}_p(t)$ and $\hat{B}_p(t)$ or equivalently $\Phi(t), \Psi(t)$ and $\Gamma(t)$ so that the quantities $e(t), \Phi(t), \Psi(t), \Gamma(t)$ tend to zero as $t \to \infty$. We choose the adaptive laws to be

$$\dot{\hat{A}}_p(t) = \dot{\hat{\Phi}}(t) = -Pe(t)X_p^T(t)$$

$$\dot{\hat{C}}_p(t) = \dot{\hat{\Psi}}(t) = -Pe(t)f^T(X_p)$$

$$\dot{\hat{B}}_p(t) = \dot{\hat{\Gamma}}(t) = -Pe(t)g^T(u)$$

where P is a symmetric positive-definite matrix ($P > 0$), which satisfies the Lyapunov equation, namely

$$A_m^T P + PA_m = -Q$$

where Q is a positive-definite matrix ($Q > 0$). These laws can be used to ensure the global stability of the overall system with the output error tending to zero asymptotically [22]. However, Lyapunov stability analysis only assures the asymptotic convergence of the state error to zero. The convergence of the parameters to their true values depends on the persistence excitation of the input u.

V. SIMULATION RESULTS

Since the curve decomposition is inevitably noisy because of noisy data, we want to see how good the motion parameters are estimated. Simulations are performed with planar free-form objects. Boundary data are corrupted by additive noise. This is achieved by adding zero mean and variance 1 of normally distributed random numbers scaled by 0.005 to the x, y coordinates of each data point. The reason that the noise is scaled by 0.005 is to make sure that the curve fitting results are not deteriorated much by the noise level. Otherwise unbounded curves can be obtained for closed-bounded data, which will adversely affect the estimation results. We picked such a noise level to guarantee that at each sampling instant we get a reasonably good curve fit.

Closed-bounded quartic curves are first fitted to the object boundaries at each sampling instant using a fitting procedure detailed in [27]. This fitting algorithm is linear, fast, repeatable, Euclidean invariant and relatively stable, but does not necessarily provide closed- bounded fits all the time. We optimized fit parameters to yield closed-bounded fits in all simulations. Resulting quartic curves are then decomposed using the unique decomposition theorem of section III to obtain line parameters at each sampling instant. There are 3 line pairs in the decomposition of a quartic curve. For closed-bounded curves, 2 of these 3 pairs are definitely complex conjugate of each other. We picked one complex conjugate pair to construct the dynamical system given by (25) and the estimator given by (27) in Matlab/Simulink. Of course, the correspondence problem between line pairs in consecutive curves must be solved in order to implement this estimator forward in time. To establish the correct correspondence between complex conjugate line pairs in consecutive curves, real intersection points (related-points) of these complex lines are determined and used in the evaluation of defining polynomials. It is known that the correct correspondence between two sets of related-points can be established by ordering the values of defining polynomials evaluated at these related-points [5].

The stability matrix, A_m and the positive-definite matrix Q are chosen to be:

$$A_m = \begin{pmatrix} -0.5 & 0 & 0 & 0 \\ 0 & -0.5 & 0 & 0 \\ 0 & 0 & -1.0 & 0 \\ 0 & 0 & 0 & -1.0 \end{pmatrix},$$

$$Q = \begin{pmatrix} 0.5 & 0 & 0 & 0 \\ 0 & 1.0 & 0 & 0 \\ 0 & 0 & 2.0 & 0 \\ 0 & 0 & 0 & 3.0 \end{pmatrix}$$

The Lyapunov equation is solved to determine the symmetric positive-definite matrix P, which is then used in parameter update rules given in section IV. Initial values of the motion parameters are chosen at random.

A mobile cellular phone employed in analysis and its motion are depicted in Fig. 4 along with superimposed quartic curves. The parameters of the rigid motion are $a_1 = a_4 = 0$, $a_2 = -a_3 = \omega = 1$, $b_1 = 2$, $b_2 = -1$. Estimated parameters are plotted against time in Fig. 5. Note that estimated parameters converge to their true values in reasonably quick time periods with reasonably small estimation error.

Another free-form object (a typical curved object) and its motion are depicted in Fig. 6 along with superimposed quartic curves. The parameters of the rigid motion are $a_1 = a_4 = 0$, $a_2 = -a_3 = \omega = -2$, $b_1 = 4$, $b_2 = 0$. Estimated parameters are plotted against time in Fig. 7. Note again that estimates converge to their true values in a relatively short time interval with a relatively small estimation error.

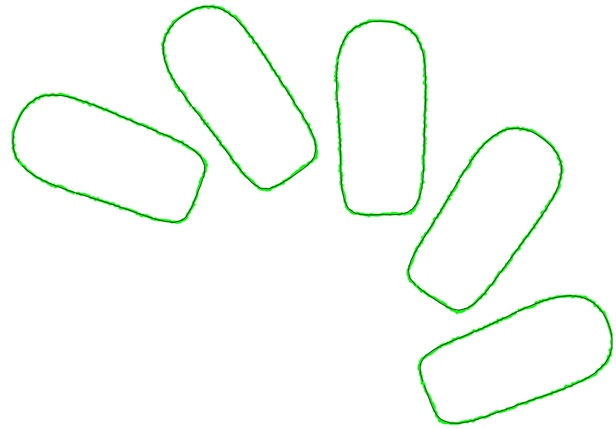

Fig. 4. Rigid Motion of a Mobile Cellular Phone in 0.6s time samples

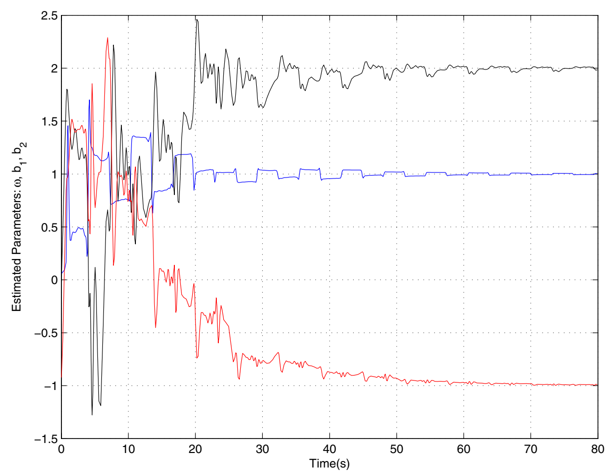

Fig. 5. Estimated parameters versus Time. True parameters are $\omega = 1$, $b_1 = 2$ and $b_2 = -1$

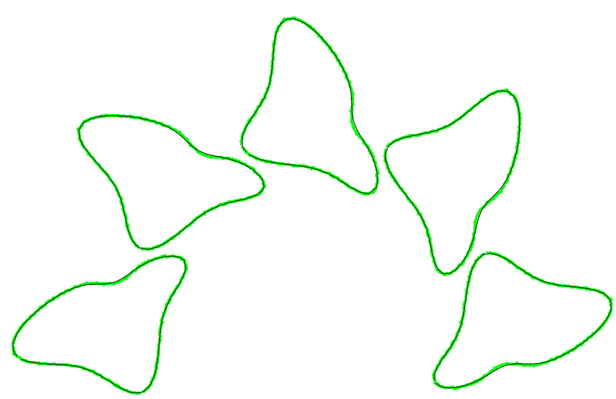

Fig. 6. Rigid Motion of a Typical Curved Object in 0.4s time samples

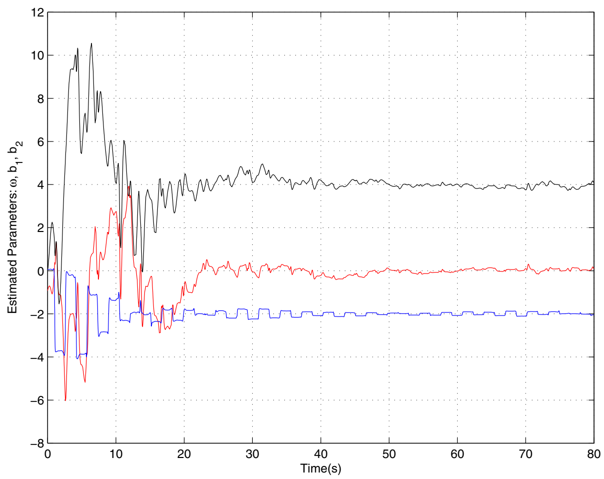

Fig. 7. Estimated parameters versus. True parameters are $\omega = -2$, $b_1 = 4$ and $b_2 = 0$

VI. CONCLUSIONS AND FUTURE WORKS

A. Conclusions

We have developed some new Riccati equations in real variables which can be used for rigid and affine motion estimation of a closed-bounded free form object whose boundary can be modelled by some plane polynomial curve. We have also employed a parameter tuning algorithm for estimating rigid motion parameters. Simulation results have shown that the parameters of a rigid motion can accurately be estimated from noisy curve data.

B. Future Works

We are investigating several observers which will enable us to estimate motion parameters of a moving curve undergoing affine motion. We are also working on possible extensions of our estimation technique to the motion of 3D free-form objects modelled by polynomial surfaces.

REFERENCES

[1] C.G. Gibson, **Elementary geometry of algebraic curves**, Cambridge University Press, Cambridge, UK, 1998.

[2] P. Frost, **An Elementary Treatise on Curve Tracing**, 4th Ed., MacMillan, London, 1918.

[3] J. Bloomenthal, **Introduction to implicit surfaces**, Kaufmann, Los Altos, CA, 1997.

[4] D. Keren et al., "Fitting curves and surfaces to data using constrained implicit polynomials," IEEE Transactions on Pattern Analysis and Machine Intelligence, Vol. 23, No. 1, January 1999.

[5] M. Unel, W. A. Wolovich, "On the construction of complete sets of geometric invariants for algebraic curves," Advances in Applied Mathematics Vol. 24, No. 1, pp. 65-87, January 2000.

[6] M. Unel, W. A. Wolovich, "A new representation for quartic curves and complete sets of geometric invariants," International Journal of Pattern Recognition and Artificial Intelligence, December 1999.

[7] M. Unel, "Polynomial decompositions for shape modeling, object recognition and alignment," PhD Thesis, Brown University, Providence, 1999.

[8] M. Unel, B. K. Ghosh, "Dynamic Models of Planar Algebraic Curves," Proceedings of IEEE CDC 2001, December 2001.

[9] J. L. Mundy, Andrew Zisserman, **Geometric invariance in computer vision**, The MIT Press, 1992.

[10] G. Taubin, D. B. Cooper, "2D and 3D object recognition and positioning with algebraic invariants and covariants," Chapter 6 of **Symbolic and Numerical Computation for Artificial Intelligence**, Academic Press, 1992.

[11] G. Taubin, F. Cukierman, S. Sullivan, J. Ponce and D.J. Kriegman, "Parameterized families of polynomials for bounded algebraic curve and surface fitting," IEEE PAMI, March, 1994.

[12] W. A. Wolovich, Mustafa Unel, "The determination of implicit polynomial canonical curves," IEEE Transactions on Pattern Analysis and Machine Intelligence, Vol. 20, No. 10, pp. 1080-1089, October 1998.

[13] W. A. Wolovich, Mustafa Unel, "Vision based system identification and state estimation," The Confluence of Vision and Control, Springer Lecture Notes in Control and Information Sciences, No. 237, pp. 171-182, 1998.

[14] A. Mitiche, S. Seida and J. K. Aggarwal, "Line based computation of structure and motion using angular invariance," Proc. Workshop on Motion: Representation and Analysis (IEEE Computer Society Press, Silver Spring, MD, 1986).

[15] Y. Liu and T. S. Huang, "A linear algorithm for motion estimation using straight line correspondences," Comput. Vision Graphics Image Process, 44 (1988).

[16] M. E. Spetsakis and J. Aloimonos, "Structure from motion using line correspondences," Internat. J. Comput. Vision, 4 (1990), pp. 171-183.

[17] M. Jankovic and B. K. Ghosh, "Visually guided ranging from observations of points, lines and curves via an identifier based nonlinear observer, Systems and Control Letters, 25, pp. 63-73, 1995.

[18] N. Andreff, B. Espiau and R. Horaud, "Visual servoing from lines," In Proc. of the 2000 IEEE International Conference on Robotics and Automation, pp. 2070-2075, San Francisco, CA, April 2000.

[19] R. Cipolla and A. Blake, "Surface shape from the deformation of apparent contours," Internat. J. Comput. Vision, vol. 9, no. 2, 1992, pp. 83-112.

[20] O. D. Faugeras, "On the motion of 3-D curves and its relationship to optical flow," in: O.D.Faugeras, ed., Proc. 1st ECCV (Springer, Berlin, 1990), pp. 107-117.

[21] O. D. Faugeras and T. Papadopoulo, "A theory of the motion fields of curves," Internat. J. Comput. Vision, vol. 10, no. 2, pp. 125-156, 1993.

[22] K. S. Narendra, A. M. Annaswamy, "Stable Adaptive Systems," 1989 by Prentice-Hall, Inc.

[23] B. K. Ghosh, H. Inaba and S. Takahashi, "Identification of Riccati dynamics under perspective and orthographic observations," IEEE Trans. on Aut. Contr., vol. 45, no. 7, July 2000, pp. 1267-1278.

[24] B. K. Ghosh, M. Jankovic and Y. T. Wu, "Perspective problems in system theory and its application to machine vision," Journal of mathematical systems, estimation and control, vol. 4, no. 1, 1994, pp. 3-38.

[25] Y. T. Wu, Estimating three dimensional motion parameters from feature based image sequence: A perspective systems approach, Ph.D. Dissertation, Washington University, Saint Louis, MO, Dec. 1991.

[26] B. K. Ghosh and E. P. Loucks, " A perspective theory for motion and shape estimation in machine vision," SIAM J. Contr. Optim., vol. 33, no. 5, pp. 1530-1559, 1995.

[27] Z. Lei, M. M. Blane and D. B. Cooper, "3L Fitting of Higher Degree Implicit Polynomials," In proceedings of Third IEEE Workshop on Applications of Computer Vision, pp. 148-153, Florida 1996.